CHALMERS
UNIVERSITY OF TECHNOLOGY

GOSPA and T-GOSPA quasi-metrics for evaluation of multi-object tracking algorithms

Citation for the original published paper (version of record):
Garca-Fernandez, A., Gu, J., Svensson, L. et al (2026). GOSPA and T-GOSPA quasi-metrics for evaluation of multi-object tracking algorithms. IEEE Transactions on Aerospace and Electronic Systems, 62: 9631-9644. http://dx.doi.org/10.1109/TAES.2026.3686336

(article starts on next page)

GOSPA and T-GOSPA Quasi-Metrics for Evaluation of Multiobject Tracking Algorithms

ÁNGEL F. GARCÍA-FERNÁNDEZ
Universidad Politécnica de Madrid, Madrid, Spain

JINHAO GU
University of Liverpool, Liverpool, U.K.

LENNART SVENSSON
Chalmers University of Technology, Gothenburg, Sweden

YUXUAN XIA, Member, IEEE
Shanghai Jiao Tong University, Shanghai, China

JAN KREJČÍ
OLIVER KOST
ONDŘEJ STRAKA
University of West Bohemia, Pilsen, Czech Republic

Received 28 December 2025; accepted 18 April 2026. Date of publication 22 April 2026; date of current version 22 May 2026.

DOI. No. 10.1109/TAES.2026.3686336

Refereeing of this contribution was handled by M. Ulmke.

This work was supported by the Spanish Ministry of Science, Innovation, and Universities, under Grant PID2024-158149OB-C21.

Authors' addresses: Ángel F. García-Fernández is with the Information Processing and Telecommunications Center, ETSI de Telecomunicación, Universidad Politécnica de Madrid, 28040 Madrid, Spain, E-mail: (angel.garcia.fernandez@upm.es); Jinhao Gu is with the Department of Electrical Engineering and Electronics, University of Liverpool, L69 3GJ Liverpool, U.K., E-mail: (jinhgu@liverpool.ac.uk); Lennart Svensson is with the Department of Electrical Engineering, Chalmers University of Technology, SE-412 96 Gothenburg, Sweden, E-mail: (lennart.svensson@chalmers.se); Yuxuan Xia is with the Department of Automation and Intelligent Sensing, Shanghai Jiao Tong University, Shanghai, 200240, China, E-mail: (yuxuan.xia@sjtu.edu.cn), Jan Krejcí, Oliver Kost, and Ondřej Straka are with the Department of Cybernetics, University of West Bohemia, 306 14 Pilsen, Czech Republic, E-mail: (jkrejci@kky.zcu.cz; kost@kky.zcu.cz; straka30@kky.zcu.cz). *(Corresponding author: Ángel F. García-Fernández.)*

This article has supplementary downloadable material available at https://doi.org/10.1109/TAES.2026.3686336, provided by the authors.

This article introduces two quasi-metrics for performance assessment of multiobject tracking (MOT) algorithms. One quasi-metric is an extension of the generalized optimal subpattern assignment (GOSPA) metric and measures the discrepancy between sets of objects. The other quasi-metric is an extension of the trajectory GOSPA (T-GOSPA) metric and measures the discrepancy between sets of trajectories. Similar to the GOSPA-based metrics, these quasi-metrics include costs for localization error for properly detected objects, the number of false objects and the number of missed objects. The T-GOSPA quasi-metric also includes a track switching cost. Differently from the GOSPA and T-GOSPA metrics, the proposed quasi-metrics have the flexibility of penalizing missed and false objects with different costs, and the localization costs are not required to be symmetric. We also explain how to obtain similarity score functions based on these quasi-metrics. The performance of several Bayesian MOT algorithms is assessed with the T-GOSPA quasi-metric via simulations.

I. INTRODUCTION

Multiobject tracking (MOT) consists of estimating the trajectories of a variable and an unknown number of objects using sensor measurements. MOT has a wide variety of applications, such as traffic monitoring [1], underwater surveillance [2], and space object cataloging [3]. This article considers the important topic of performance evaluation of MOT algorithms [4], [5]. That is, given a ground truth set of trajectories and the estimated sets of trajectories provided by several algorithms, the best performing algorithm is the one whose estimate is the most similar to the ground truth. Therefore, to assess MOT algorithm performance, it is necessary to establish a definition of error or distance between two sets of trajectories.

In mathematics, the notion of error or distance can be defined via metrics[1]. Metrics are nonnegative functions that meet three properties: identity, symmetry, and triangle inequality [6]. These properties ensure that the notion of distance is intuitive and they are the foundation of important properties for mathematical analysis, such as the concept of metric spaces. The triangle inequality guarantees that distances between points follow a consistent and logical pattern. That is, it prevents cases where the direct distance between two endpoints is greater than the sum of the distances between any intermediate points. We proceed to review the literature on performance evaluation for MOT.

Multiobject filtering is a subproblem of MOT in which the goal is to estimate the current set of objects, rather than the set of trajectories. A widely used metric for sets of objects is the optimal subpattern assignment (OSPA) metric [7], [8]. Other metrics for sets of objects are the cardinalized optimal linear assignment (COLA) metric [9], [10] (which is equal to the unnormalized OSPA (UOSPA) metric [11, eq. (44)] divided by its cardinality mismatch parameter c), the Hausdorff and Wasserstein metrics [12], and the complete OSPA metric [13]. However, none of the above mentioned metrics penalize all the factors that are considered of interest in MOT: localization errors

[1]The terms distance and metric are sometimes used interchangeably. In this article, a distance refers to a function that may not fulfill all the mathematical properties required of a metric.

for detected objects, the number of missed objects, and the number of false objects, in the sense that an increase in any of these factors implies an increase in the metric value. For instance, in some situations, we can add false objects to the estimated set of objects, but the values of the above metrics remain unchanged [14, Example 2]. These factors can be penalized with the generalized optimal subpattern assignment (GOSPA) metric [14].

In MOT, apart from penalizing the above factors, it is relevant to penalize track switches since the estimated trajectories of different objects may be swapped at some point in time. In computer vision, there are several methods to assess the accuracy of the estimated trajectories, including the number of track switches, which can be lowered by object reidentification modules [15], [16], [17]. One example is the multiple object tracking accuracy (MOTA) score [18], and its variations [19]. MOTA is based on obtaining a heuristic matching between the ground truth states and the estimated object states at each time step. With this matching, the MOTA score is defined based on the number of track switches, missed objects, and false objects, but not on the localization errors for matched objects [18]. The MOTA score indicates similarity, takes values in the interval $(-\infty, 1]$, and is nonsymmetric. As MOTA does not consider localization errors, these are usually measured in this setting by calculating a companion index, the multiple object tracking precision (MOTP). The MOTP was originally defined as an error [18], but it can also be defined as a similarity with a minor modification [20].

Another similarity score for MOT used in computer vision, taking values in [0, 1], is the higher order tracking accuracy (HOTA) score [20]. The HOTA score for a given similarity threshold α (HOTA_α) is based on solving an external assignment problem (e.g., an assignment problem with another cost function) at each time step. The solutions of the external assignment problems are then used to calculate the HOTA_α score, which depends on the number of missed objects, false objects, and track switches, but it does not depend on localization errors for properly detected objects. The overall HOTA is then obtained by averaging HOTA_α over multiple similarity thresholds, to indirectly account for localization errors. However, MOTA, MOTP and HOTA are not mathematical metrics, as they do not meet the identity and triangle inequality properties.

To define a metric for sets of trajectories, one solution is to first determine a base distance for trajectories and then apply the OSPA metric. This procedure results in the $\text{OSPA}^{(2)}$ metric [21]. It is also directed to prove that an unnormalized version of the $\text{OSPA}^{(2)}$ metric, referred to as $\text{UOSPA}^{(2)}$, is also a metric. $\text{OSPA}^{(2)}$ and $\text{UOSPA}^{(2)}$ associate estimated trajectories to ground truth trajectories, but the association remains fixed across time. Therefore, $\text{OSPA}^{(2)}$ and $\text{UOSPA}^{(2)}$ do not include penalties for track switches, and do not penalize the number of missed and false objects, either [22].

Bento and Zhu's [23] metrics are mathematically consistent metrics for sets of trajectories and penalize track switches, although they require the introduction of $*$-trajectories to ensure that the two sets have the same number of elements. The extension of the GOSPA metric to sets of trajectories, termed trajectory GOSPA (T-GOSPA) metric, was presented in [24] to penalize localization errors, the number of missed and false objects, and the number of track switches. T-GOSPA works by assigning at each time step trajectories in both sets, while allowing for the possibility of leaving trajectories unassigned. T-GOSPA was extended to have time-weighted costs in [22]. Both T-GOSPA and Bento's metrics have linear programming (LP) relaxation variants, which are also metrics and are faster to compute. Approximate, fast implementations of the T-GOSPA metric for large tracking scenarios based on unbalanced multimarginal optimal transport and graph structured optimal transport have been recently proposed in [25] and [26].

A property of the GOSPA and T-GOSPA metrics is that missed and false objects are penalized with the same cost, to ensure the symmetry property. The previous distances and similarity scores also share this property. However, there are some applications in which it is more suitable to have different costs for missed and false objects. For instance, in classic radar detector design, one typically sets a very low probability of false alarm and then maximizes the probability of detection using a Neyman–Pearson test [27, Ch. 10]. With this design, the cost of a false object is higher than the cost of a missed object. In other applications, it is crucial not to miss any objects, for instance, in self-driving vehicles, uncrewed surface vessels, or satellite collision avoidance systems. Hence, it is desirable to assess algorithms with a higher penalty for missed objects than for false objects.

To achieve this flexibility in the costs for missed and false objects, it is necessary to develop distance functions that are nonsymmetric. Distances that meet the metric properties except the symmetry property are called quasimetrics (q-metrics) [28], [29], [30]. Q-metrics have been used in several applications: similarity search in protein datasets [31], reinforcement learning [32], and q-metric learning [33]. A q-metric for MOT with continuous trajectories has been proposed in [34], the Star-ID metric. The Star-ID metric penalizes trajectory segments not assigned to other trajectories as well as full unassigned trajectories, with costs depending on the segment/trajectory lengths. However, the Star-ID metric has the constraint of requiring fixed assignments of trajectories across time, and therefore, it does not include costs for track switches. In addition, it is not applicable to the standard MOT problems that estimate trajectories in discrete time.

This article proposes q-metrics for multiobject filtering and MOT that penalize the aspects of interest in MOT: localization errors, number of false objects, number of missed objects, and track switches. The proposed GOSPA and T-GOSPA q-metrics are designed based on the GOSPA and T-GOSPA metrics and use a base distance that is a q-metric and incorporate an additional parameter $\rho \in (0, 1)$ that controls the penalties for false and missed objects. In addition, motivated by the use of similarity score functions, taking values in [0, 1], to measure performance in MOT in

computer vision, we define and derive score functions based on the proposed q-metrics to measure similarity between sets of objects and trajectories.

The contributions of this article are as follows.

1) Development of the GOSPA q-metric[2] for sets of objects for performance evaluation of multiobject filters with different costs for missed and false objects, including the proofs of the q-metric properties.
2) Development of the T-GOSPA q-metric for sets of trajectories for performance evaluation of MOT algorithms with different costs for missed and false objects, including the proofs of the q-metric properties.
3) Derivation of three properties of the GOSPA and T-GOSPA q-metrics related to the q-metric parameter ρ.
4) Definition and derivation of q-metric-based score functions, based on GOSPA and T-GOSPA, to measure the similarity between sets of objects and trajectories.
5) Extensions of the GOSPA and T-GOSPA q-metrics, and their associated score functions, to random finite sets (RFSs) [35].

This article also provides simulation results evaluating state-of-the-art Bayesian MOT algorithms via the T-GOSPA q-metric.

The rest of this article is organized as follows. Section II presents the required background. Sections III and IV introduce the GOSPA and T-GOSPA q-metrics, respectively. The derivation of q-metric-based score functions is addressed in Section V. The extensions of the q-metrics to RFSs are provided in Section VI. Simulation results are analyzed via the T-GOSPA q-metric in Section VII. Finally, Section VIII concludes this article.

II. BACKGROUND

This section introduces the variables we consider (see Section II-A), the definitions of metrics and q-metrics (see Section II-B), and the GOSPA metric (see Section II-C).

A. Variables

We denote a single object state as $x \in \mathbb{X}$, with $\mathbb{X}$ being the single-object space. The single-object space is typically $\mathbb{X} = \mathbb{R}^{n_x}$, and contains information on the object kinematics, such as position and velocity, and it can also include discrete variables, such as object type. A set of objects is then represented as $\mathbf{x} = \{x_1, \ldots, x_{n_\mathbf{x}}\}$, and its cardinality is $|\mathbf{x}| = n_\mathbf{x}$ [35].

The trajectory of an object is denoted by $X = (\omega, x^{1:\nu})$. Here, ω is the trajectory start time step, ν is the trajectory duration, and $x^{1:\nu} = (x^1, \ldots, x^\nu)$ is the sequence of object states of this trajectory [36]. We focus on trajectories contained in a time window from time step 1 to time step T, such that $1 \leq \omega \leq T$ and $1 \leq \nu \leq T - \omega + 1$. A set of object trajectories is denoted by $\mathbf{X} = \{X_1, \ldots, X_{n_\mathbf{X}}\}$, with cardinality $|\mathbf{X}| = n_\mathbf{X}$.

B. Metric and Q-Metrics

A metric on a given space Υ is a nonnegative function $d(\cdot, \cdot) : \Upsilon \times \Upsilon \to [0, \infty)$ that meets the following properties for any $\mathbf{X}, \mathbf{Y}, \mathbf{Z} \in \Upsilon$ [6].

1) $d(\mathbf{X}, \mathbf{Y}) = 0$ if and only if $\mathbf{X} = \mathbf{Y}$ (identity).
2) $d(\mathbf{X}, \mathbf{Y}) = d(\mathbf{Y}, \mathbf{X})$ (symmetry).
3) $d(\mathbf{X}, \mathbf{Y}) \leq d(\mathbf{X}, \mathbf{Z}) + d(\mathbf{Z}, \mathbf{Y})$ (triangle inequality).

A q-metric is a nonnegative function $d(\cdot, \cdot) : \Upsilon \times \Upsilon \to [0, \infty)$ that meets the identity and triangle inequality properties, but it does not need to meet the symmetry property [28], [29], [30].

The triangle inequality is a key property to define distances between points in a space, and also to measure the error of estimators. For example, let us illustrate this with the following example, adapted from [35, Sect. 6.2.1]. Let $\mathbf{X}$ be the ground truth and let $\mathbf{Y}_1$ and $\mathbf{Y}_2$ be two estimates. If estimate $\mathbf{Y}_1$ is close to $\mathbf{X}$ and estimate $\mathbf{Y}_2$ is close to $\mathbf{Y}_1$, that is, both $d(\mathbf{X}, \mathbf{Y}_1)$ and $d(\mathbf{Y}_1, \mathbf{Y}_2)$ are small, then $\mathbf{Y}_2$ should be close to $\mathbf{X}$ implying that $d(\mathbf{X}, \mathbf{Y}_2)$ is small as well. This property is ensured for metrics and q-metrics by the triangle inequality.

In the rest of this article, the ground truth set of objects and the ground truth set of trajectories are denoted by $\mathbf{x}$ and $\mathbf{X}$, respectively. The corresponding estimates provided by a certain algorithm are denoted by $\mathbf{y}$ and $\mathbf{Y}$.

C. GOSPA Metric

This section reviews the GOSPA metric (for parameter $\alpha = 2$, as defined in [14]), as it is the point of reference for the q-metrics. The ground truth sets of objects and its estimate are written as $\mathbf{x} = \{x_1, \ldots, x_{n_\mathbf{x}}\}$ and $\mathbf{y} = \{y_1, \ldots, y_{n_\mathbf{y}}\}$. The GOSPA metric looks for an optimal assignment set between the objects in $\mathbf{x}$ and the elements in $\mathbf{y}$, with the assignment set indicating what objects are matched, and which ones are left without assignment. An assignment set θ meets $\theta \subseteq \{1, .., n_\mathbf{x}\} \times \{1, .., n_\mathbf{y}\}$, $(i, j), (i, j') \in \theta$ implies $j = j'$, and $(i, j), (i', j) \in \theta$ implies $i = i'$. The set of all possible assignment sets is $\Gamma_{\mathbf{x},\mathbf{y}}$, such that $\theta \in \Gamma_{\mathbf{x},\mathbf{y}}$.

DEFINITION 1: For a base metric $d_b(\cdot, \cdot)$ on the single-object space $\mathbb{X}$, a maximum localization cost parameter $c > 0$, and a real parameter p with $1 \leq p < \infty$, the GOSPA metric between sets $\mathbf{x}$ and $\mathbf{y}$ of objects is [14, Prop. 1]

$$d_p^{(c)}(\mathbf{x}, \mathbf{y}) = \min_{\theta \in \Gamma_{\mathbf{x},\mathbf{y}}} \left(\sum_{(i,j)\in\theta} d_b\left(x_i, y_j\right)^p + \frac{c^p}{2}\left(|\mathbf{x}| + |\mathbf{y}| - 2|\theta|\right) \right)^{1/p}. \quad (1)$$

[2]MATLAB and Python implementations of the GOSPA and T-GOSPA q-metrics are available at https://github.com/Agarciafernandez/MTT and https://github.com/Agarciafernandez/T-GOSPA-metric-python.

The first term in (1) is the sum of the localization costs (to the pth power) for pairs of assigned objects, whose indices are $(i, j) \in \theta$. These are the objects in $\mathbf{x}$ that have been properly detected and, therefore, have an associated object in the estimated set $\mathbf{y}$. The terms $\frac{c^p}{2}(|\mathbf{x}| - |\theta|)$ and $\frac{c^p}{2}(|\mathbf{y}| - |\theta|)$ are the penalties (to the pth power) for the number of missed and false objects. Each missed and each false object contribute with a cost $\frac{c^p}{2}$ to the overall cost (before taking the pth root).

III. GOSPA Q-METRIC

This section introduces the GOSPA q-metric in Section III-A. Then, we present representative examples to illustrate how the q-metric works in Section III-B. The choice of parameters is explained in Section III-C. Three properties of the GOSPA q-metric are provided in Section III-D.

A. Definition

The design principles (DPs) of the GOSPA q-metric are are as follows.

1) *DP1:* The q-metric returns a higher value if the estimated set of targets includes more false objects, misses more real objects, or has higher estimation errors for properly detected objects.
2) *DP2:* Clear interpretability by the decomposition of the q-metric into costs penalising the number of false objects, the number of missed objects, and the estimation errors for properly detected objects.
3) *DP3:* The relative weighting of missed and false object costs can be adapted.

DP1 and DP2 are also the DPs of the GOSPA metric. Then, the definition of the GOSPA q-metric is the following.

DEFINITION 2: For a base q-metric $d_b(\cdot, \cdot)$ in the single-object space $\mathbb{X}$, a maximum localization cost parameter $c > 0$, real parameter p with $1 \leq p < \infty$, and q-metric parameter $\rho \in (0, 1)$, the GOSPA q-metric $d_p^{(c,\rho)}(\cdot, \cdot)$ between two sets $\mathbf{x}$ and $\mathbf{y}$ of objects is

$$d_p^{(c,\rho)}(\mathbf{x}, \mathbf{y}) = \min_{\theta \in \Gamma_{\mathbf{x},\mathbf{y}}} \left(\sum_{(i,j)\in\theta} d_b^p\left(x_i, y_j\right) + \rho c^p \left(|\mathbf{y}| - |\theta|\right) + (1-\rho)\, c^p \left(|\mathbf{x}| - |\theta|\right) \right)^{1/p}. \quad (2)$$

The differences between the GOSPA q-metric (2) and the GOSPA metric in (1) are that $d_b(\cdot, \cdot)$ is allowed to be a q-metric, the penalty (to the pth power) for a false object is $c_f^p = \rho c^p$ and the penalty (to the pth power) for a missed object is $c_m^p = (1-\rho)c^p$, where $\rho \in (0, 1)$ is the fraction of the maximum localization error c^p that represents a false object cost (to the pth power). For $\rho = 1/2$ and $d_b(\cdot, \cdot)$ being a metric, the GOSPA q-metric becomes the GOSPA metric.

An alternative parameterization of the GOSPA q-metric is to define it in terms of c_f and c_m, instead of c and ρ.

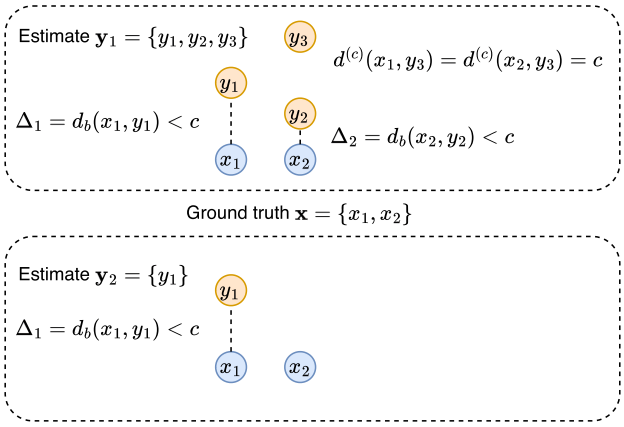

Fig. 1. Two estimated sets of objects $\mathbf{y}_1$ and $\mathbf{y}_2$ of the ground truth $\mathbf{x}$. The dashed lines represent assignments between the elements of the ground truth and the estimate. Estimate $\mathbf{y}_1$ has two properly detected objects with localization errors Δ_1 and Δ_2 and a false object. Estimate $\mathbf{y}_2$ has one properly detected object with localization error Δ_1 plus a missed object.

TABLE I
Distances/scores for the Example in Fig. 1 When Some Estimates are Close or All of Them are Far Away

	Close		Far away	
	$\mathbf{y}_1$	$\mathbf{y}_2$	$\mathbf{y}_1$	$\mathbf{y}_2$
GOSPA	$\Delta_1 + \Delta_2 + \rho c$	$\Delta_1 + (1-\rho)\, c$	$(2+\rho)\, c$	$(2-\rho)\, c$
OSPA	$\frac{\Delta_1+\Delta_2+c}{3}$	$\frac{\Delta_1+c}{2}$	c	c
UOSPA	$\Delta_1 + \Delta_2 + c$	$\Delta_1 + c$	$3c$	$2c$
COLA	$\frac{\Delta_1+\Delta_2+c}{c}$	$\frac{\Delta_1+c}{c}$	3	2
HOTA(↑)	2/3	1/2	0	0

The conversion between both parameterizations is straightforward. We use the parameterization in terms of c and ρ as parameter c is the maximum localization cost, which enables that a pair of objects can be assigned to each other, which is an intuitive concept. Parameter c is also used in the GOSPA metric and is used in the triangle inequality proof.

It is direct to check the nonnegativity and identity properties of (2). The triangle inequality is proved in Appendix B of the Supplementary Material. The GOSPA q-metric can be computed in polynomial time since it can be written as a 2-D assignment problem [37].

B. Examples

We demonstrate the operation of the GOSPA q-metric using the examples presented in Fig. 1. For clarity, we focus on the case where $p = 1$. The GOSPA q-metric, OSPA, UOSPA, COLA, and HOTA values for the estimates $\mathbf{y}_1$ and $\mathbf{y}_2$ are given in Table I ("Close" columns). For the GOSPA metric ($\rho = 1/2$), $\mathbf{y}_2$ is more accurate than $\mathbf{y}_1$. This is because both estimates detect an object with the same localization error, and have either a missed or a false object, but $\mathbf{y}_1$ has an additional localization error. For UOSPA/COLA, $\mathbf{y}_2$ is also more accurate than $\mathbf{y}_1$, while for OSPA, the ranking depends on the localization error Δ_2. On the other hand, HOTA indicates that $\mathbf{y}_1$ is more accurate than $\mathbf{y}_2$. For the GOSPA q-metric, the estimate $\mathbf{y}_2$ is more

accurate than $\mathbf{y}_1$ if

$$\rho > \frac{1}{2} - \frac{\Delta_2}{2c}. \tag{3}$$

That is, the parameter ρ, which is proportional to the false object cost, must be sufficiently high such that $\mathbf{y}_2$ is considered better than $\mathbf{y}_1$. This is reasonable as $\mathbf{y}_2$ misses an object while $\mathbf{y}_1$ has a false object and one more estimate associated to a true object, so a high enough ρ makes $\mathbf{y}_2$ a better estimate. On the contrary, for sufficiently small ρ, the GOSPA q-metric indicates that $\mathbf{y}_1$ is more accurate than $\mathbf{y}_2$, since the false object is penalized less.

Let us now consider the case where $\Delta_1 > c$ and $\Delta_2 > c$. That is, all estimates are far away from the real-object locations. In this case, the optimal assignments are not the ones shown in Fig. 1 as it is the best to leave all objects unassigned. This implies that $\mathbf{y}_1$ misses two objects and declares three false objects. On the other hand, $\mathbf{y}_2$ misses two objects and contains one false object. The resulting errors are shown in Table I ("Far away" columns). HOTA and OSPA indicate that both estimates are equally good, which imply that they do not meet DP1. GOSPA q-metric for all values of $\rho \in (0, 1)$, UOSPA and COLA indicate that $\mathbf{y}_2$ is more accurate than $\mathbf{y}_1$, meeting DP1. An example where OSPA–UOSPA–COLA do not meet DP1 is given in [14, Example 2].

C. Choice of Parameters

The parameters c and p are chosen as in the GOSPA metric. That is, parameter c is the maximum localization error and is chosen depending on the application. One true object state x and an estimate y can only be assigned to each other if their distance according to the base q-metric is lower than c. Parameter p can be chosen to adapt how outliers are penalized, with a higher value of p penalizing outliers more [8], [14].

In most applications, the base q-metric $d_b(\cdot, \cdot)$ will typically be chosen to be a metric. For example, for point objects (which do not have an extent), one can use the Euclidean distance. For extended objects modeled by ellipses, one can use the Gaussian Wasserstein distance [38]. Parameter ρ can be chosen taking into account how much a false object should be penalized compared to a missed object in a given application. This leads to the following lemma.

LEMMA 3 If the cost of a false object (to the pth power) is $\nu \in (0, \infty)$ times the cost (to the pth power) of a missed object ($c_f^p = \nu c_m^p$), then the GOSPA q-metric parameter ρ is

$$\rho = \frac{\nu}{\nu + 1}. \tag{4}$$

The proof of this lemma follows from the definitions of c_f^p and c_m^p in the paragraph after (2).

D. Properties

This section provides several properties of the GOSPA q-metric. It is direct to prove the following lemma.

LEMMA 4 If $d_b(\cdot, \cdot)$ is a metric, then the GOSPA q-metric meets

$$d_p^{(c,\rho)}(\mathbf{x}, \mathbf{y}) = d_p^{(c,1-\rho)}(\mathbf{y}, \mathbf{x}). \tag{5}$$

In addition, we prove in Appendix C-A of the Supplementary Material the following result.

LEMMA 5 The optimal assignment set (or the optimal permutation) of the GOSPA q-metric does not depend on ρ.

This result implies that for different values of ρ, the localization costs remain unchanged, but we have different missed and false object costs, and a different overall metric value. In addition, Lemma 5 implies that if $d_b(\cdot, \cdot)$ is a metric, then the optimal assignment set is the same as in the GOSPA metric.

The symmetrization property of the GOSPA q-metric is stated in the following lemma (proved in Appendix C-B of the Supplementary Material).

LEMMA 6 If $d_b(\cdot, \cdot)$ is a metric, then the GOSPA metric $d_p^{(c,1/2)}(\mathbf{x}, \mathbf{y})$ is recovered with the following symmetrization of the GOSPA q-metric

$$d_p^{(c,1/2)}(\mathbf{x}, \mathbf{y}) = \left[\frac{1}{2}\left(d_p^{(c,\rho)}(\mathbf{x}, \mathbf{y})^p + d_p^{(c,\rho)}(\mathbf{y}, \mathbf{x})^p\right)\right]^{1/p}. \tag{6}$$

IV. T-GOSPA Q-METRICS

This section presents the T-GOSPA q-metrics for sets of trajectories. We first cover the GOSPA q-metric for sets of objects with at most one element (see Section IV-A). We then present the T-GOSPA q-metric for sets of trajectories in terms of multidimensional assignments across time (see Section IV-B). Then, we introduce the relaxation of the multidimensional assignment T-GOSPA q-metric via LP (see Section IV-C). Examples illustrating the T-GOSPA q-metric results are presented in Section IV-D. Finally, three properties of the T-GOSPA q-metric are presented (see Section IV-E).

A. Preliminaries

A building block of the T-GOSPA q-metric is the GOSPA q-metric for sets of objects with at most one element. Given two sets of objects $\mathbf{x}$ and $\mathbf{y}$ such that $|\mathbf{x}| \leq 1$ and $|\mathbf{y}| \leq 1$, the GOSPA q-metric (2) becomes

$$d_p^{(c,\rho)}(\mathbf{x}, \mathbf{y}), \triangleq \begin{cases} \min\left(c, d_b(x, y)\right), & \mathbf{x} = \{x\}, \mathbf{y} = \{y\} \\ \rho^{1/p} c, & \mathbf{x} = \emptyset, \mathbf{y} = \{y\} \\ (1-\rho)^{1/p} c, & \mathbf{x} = \{x\}, \mathbf{y} = \emptyset \\ 0, & \mathbf{x} = \mathbf{y} = \emptyset. \end{cases} \tag{7}$$

B. Multidimensional Assignment T-GOSPA Q-Metric

This section presents the T-GOSPA q-metric as the solution to a multidimensional assignment problem. The DPs of the T-GOSPA q-metric are DP3 and the following.

1) *DP4:* The q-metric gives a higher value when the estimated set of trajectories includes more false objects, misses more real objects, has higher estimation errors for properly detected objects, or has higher number of track switches.
2) *DP5:* Clear interpretability by the decomposition of the q-metric into costs penalizing the number of false objects, the number of missed objects, the number of track switches, and the estimation errors for properly detected objects.

DP4 and DP5 are the same DPs as of the T-GOSPA metric. The ground truth sets of trajectories and its estimate are written as $\mathbf{X} = \{X_1, \ldots, X_{n_\mathbf{X}}\}$ and $\mathbf{Y} = \{Y_1, \ldots, Y_{n_\mathbf{Y}}\}$. For the trajectories X_i and Y_j, the corresponding set of objects at time step k are represented by $\mathbf{x}_i^k$ and $\mathbf{y}_j^k$. It is met that $|\mathbf{x}_i^k| \leq 1$ and $|\mathbf{y}_j^k| \leq 1$ as these sets are either empty, if the corresponding trajectory does not have an object state at time step k, or have a single element. The number of objects in $\mathbf{X}$ that are present at time step k is denoted $n_\mathbf{X}^k = \sum_{i=1}^{n_\mathbf{X}} |\mathbf{x}_i^k|$. A similar notation, $n_\mathbf{Y}^k$, is used for $\mathbf{Y}$.

In the trajectory q-metrics, we make assignments at each time step between the trajectories in $\mathbf{X}$ and those in $\mathbf{Y}$. That is, at each time step, each set $\mathbf{x}_i^k$ is associated to a set $\mathbf{y}_j^k$ or is left without an assignment.

To represent these assignments, we can use assignment vectors as follows. An assignment vector at time step k is written as $[\pi_1^k, \ldots, \pi_{n_\mathbf{X}}^k]$, with $n_\mathbf{X}$ being its length. If its ith entry $\pi_i^k = j$, with $j \in \{1, \ldots, n_\mathbf{Y}\}$, it means that $\mathbf{x}_i^k$ is assigned to $\mathbf{y}_j^k$. As there can be at maximum one $\mathbf{x}_i^k$ assigned to $\mathbf{y}_j^k$, and the other way round, the assignment vector has the constraint that $\pi_i^k = \pi_{i'}^k = j > 0$ implies $i = i'$. A value $\pi_i^k = 0$ implies that $\mathbf{x}_i^k$ is unassigned. The set of all these possible assignment vectors is then written as $\Pi_{\mathbf{X},\mathbf{Y}}$.

DEFINITION 7 Given a base q-metric $d_b(\cdot,\cdot)$ in the single-object space $\mathbb{X}$, a maximum localization cost $c > 0$, a real parameter p with $1 \leq p < \infty$, a track switching penalty $\gamma > 0$, and q-metric parameter $\rho \in (0, 1)$, the T-GOSPA q-metric $d_p^{(c,\rho,\gamma)}(\mathbf{X}, \mathbf{Y})$ between two sets $\mathbf{X}$ and $\mathbf{Y}$ of trajectories is

$$d_p^{(c,\rho,\gamma)}(\mathbf{X},\mathbf{Y}) = \min_{\substack{\pi^k \in \Pi_{\mathbf{X},\mathbf{Y}} \\ k=1,\ldots,T}} \left(\sum_{k=1}^{T} d_{\mathbf{X},\mathbf{Y}}^k \left(\mathbf{X},\mathbf{Y},\pi^k\right)^p + \sum_{k=1}^{T-1} s_{\mathbf{X},\mathbf{Y}} \left(\pi^k, \pi^{k+1}\right)^p \right)^{1/p} \tag{8}$$

where

$$d_{\mathbf{X},\mathbf{Y}}^k \left(\mathbf{X},\mathbf{Y},\pi^k\right)^p = \sum_{(i,j)\in\theta^k(\pi^k)} d_p^{(c,\rho)} \left(\mathbf{x}_i^k, \mathbf{y}_j^k\right)^p + \rho c^p \left(n_\mathbf{Y}^k - \left|\theta^k\left(\pi^k\right)\right|\right) + (1-\rho)\, c^p \left(n_\mathbf{X}^k - \left|\theta^k\left(\pi^k\right)\right|\right) \tag{9}$$

includes the costs (to the pth power) for properly detected objects (first line), false objects (second line), and missed objects (third line) at time step k, and $d_p^{(c,\rho)}(\cdot,\cdot)$ is the GOSPA q-metric in (7)

$$\theta^k\left(\pi^k\right) = \left\{ (i, \pi_i^k) : i \in \{1, \ldots, n_\mathbf{X}\}, \left|\mathbf{x}_i^k\right| = \left|\mathbf{y}_{\pi_i^k}^k\right| = 1,\ d_p^{(c,\rho)}\left(\mathbf{x}_i^k, \mathbf{y}_{\pi_i^k}^k\right) < c \right\} \tag{10}$$

and the track switch penalty (to the pth power) between time step k and $k+1$ is

$$s_{\mathbf{X},\mathbf{Y}}\left(\pi^k, \pi^{k+1}\right)^p = \gamma^p \sum_{i=1}^{n_\mathbf{X}} s\left(\pi_i^k, \pi_i^{k+1}\right) \tag{11}$$

$$s\left(\pi_i^k, \pi_i^{k+1}\right) = \begin{cases} 0, & \pi_i^k = \pi_i^{k+1} \\ 1, & \pi_i^k \neq \pi_i^{k+1},\ \pi_i^k \neq 0,\ \pi_i^{k+1} \neq 0 \\ \frac{1}{2}, & \text{otherwise.} \end{cases}$$

The proof that $d_p^{(c,\rho,\gamma)}(\cdot,\cdot)$ in Definition 7 is a q-metric, meeting the properties indicated in Section II-B, will be included as part of the proof for its LP version in the next subsection. The T-GOSPA q-metric above (and also the LP relaxation version in the next subsection) is simply using the GOSPA q-metric (7) inside the original T-GOSPA metric in [24]. The T-GOSPA metric is obtained by setting $\rho = 1/2$ provided that $d_b(\cdot,\cdot)$ is a metric. Apart from the costs for false, missed, and localization errors (already present in the GOSPA q-metric), the T-GOSPA q-metric also introduces a cost for track switches that remains symmetric in the q-metric, to enable the LP relaxation. Equation (9) corresponds to the GOSPA q-metric, but with the object-level assignment set $\theta^k(\pi^k)$ being determined by the trajectory-level association π^k. For two objects to be assigned in $\theta^k(\pi^k)$, their base q-metric must be smaller than c, as indicated by (10). For one time step $T = 1$, the T-GOSPA q-metric becomes the GOSPA q-metric. Parameter ρ in the T-GOSPA q-metric can be chosen as in the GOSPA q-metric, see Section III-C. The rest of the parameters can be chosen as in the T-GOSPA metric [24].

C. LP T-GOSPA q-Metric

To define the LP T-GOSPA q-metric, we first need to provide some additional notations. The transpose of a matrix A is written as $A^\dagger$. The assignments of the T-GOSPA q-metric can be written using binary matrices [24]. A matrix W^k of size $(n_\mathbf{X}+1) \times (n_\mathbf{Y}+1)$ that represents assignments between $\mathbf{X}$ and $\mathbf{Y}$ meets the properties

$$W^k(i,j) \in \{0,1\} \quad \forall\, i, j \tag{12}$$

$$\sum_{i=1}^{n_{\mathbf{X}}+1} W^k(i,j) = 1, \;\; j = 1, \ldots, n_{\mathbf{Y}} \tag{13}$$

$$\sum_{j=1}^{n_{\mathbf{Y}}+1} W^k(i,j) = 1, \;\; i = 1, \ldots, n_{\mathbf{X}} \tag{14}$$

$$W^k(n_{\mathbf{X}}+1, n_{\mathbf{Y}}+1) = 0 \tag{15}$$

where $W^k(i,j)$ is the (i,j) element of matrix W^k. A value $W^k(i,j) = 1$ means that $\mathbf{x}_i^k$ is assigned to $\mathbf{y}_j^k$ and a value $W^k(i,j) = 0$ means that $\mathbf{x}_i^k$ is not assigned to $\mathbf{y}_j^k$. In addition, if $\mathbf{x}_i^k$ is left without assignment, then $W^k(i, n_{\mathbf{Y}}+1) = 1$. Similarly, if $\mathbf{y}_j^k$ is left without assignment, then $W^k(n_{\mathbf{X}}+1, j) = 1$. The set of binary matrices that meet (12)–(15) is $\mathcal{W}_{\mathbf{X},\mathbf{Y}}$.

The LP T-GOSPA q-metric is based on changing the binary constraint (12) by a relaxed version

$$W^k(i,j) \geq 0 \quad \forall i, j. \tag{16}$$

The set of matrices that meet (13)–(15) and (16) is denoted as $\overline{\mathcal{W}}_{\mathbf{X},\mathbf{Y}}$.

PROPOSITION 8: Given a base q-metric $d_b(\cdot,\cdot)$ in the single-object space $\mathbb{X}$, a maximum localization cost $c > 0$, a real parameter p with $1 \leq p < \infty$, a track switching penalty $\gamma > 0$, and q-metric parameter $\rho \in (0,1)$, the LP relaxation $\overline{d}_p^{(c,\rho,\gamma)}(\mathbf{X},\mathbf{Y})$ of $d_p^{(c,\rho,\gamma)}(\mathbf{X},\mathbf{Y})$ is a q-metric with expression

$$\overline{d}_p^{(c,\rho,\gamma)}(\mathbf{X},\mathbf{Y}) = \min_{\substack{W^k \in \overline{\mathcal{W}}_{\mathbf{X},\mathbf{Y}} \\ k=1,\ldots,T}} \left(\sum_{k=1}^{T} \operatorname{tr}\left[\left(D_{\mathbf{X}\mathbf{Y}}^k\right)^{\dagger} W^k \right] + \frac{\gamma^p}{2} \sum_{k=1}^{T-1} \sum_{i=1}^{n_{\mathbf{X}}} \sum_{j=1}^{n_{\mathbf{Y}}} |W^k(i,j) - W^{k+1}(i,j)| \right)^{\frac{1}{p}} \tag{17}$$

where $D_{\mathbf{X},\mathbf{Y}}^k$ is a matrix of size $(n_{\mathbf{X}}+1) \times (n_{\mathbf{Y}}+1)$ whose (i,j) element is

$$D_{\mathbf{X},\mathbf{Y}}^k(i,j) = d_p^{(c,\rho)}\left(\mathbf{x}_i^k, \mathbf{y}_j^k\right)^p \tag{18}$$

where we recall that $d_p^{(c,\rho)}(\cdot,\cdot)$ is the GOSPA q-metric (7), and $\mathbf{x}_{n_{\mathbf{X}}+1}^k = \emptyset$ and $\mathbf{y}_{n_{\mathbf{Y}}+1}^k = \emptyset$.

The identity property of the q-metric is direct and the triangle inequality is proved in Appendix D of the Supplementary Material. It should be noted that if instead of optimizing over $\overline{\mathcal{W}}_{\mathbf{X},\mathbf{Y}}$ in (17), we optimize over $\mathcal{W}_{\mathbf{X},\mathbf{Y}}$ (the nonrelaxed assignment matrices), then (17) becomes (8). In addition, as in [22], it is possible to add time weights in both (8) and (17) and the q-metric properties are preserved. The T-GOSPA q-metric (LP implementation) can be computed in polynomial time since it is an LP [39]. Clustering can also be used to speed up computation [24, Sect. IV-D]. It is also possible to obtain approximate, fast computations following the approaches in [25] and [26].

As the T-GOSPA metric, the T-GOSPA q-metric can be decomposed into different costs associated to localization errors, missed objects, false objects, and track switches [24, Sect. IV-C]. This decomposition provides a clear interpretability of the obtained results. It is also direct to apply the q-metric with trajectories with gaps [24].

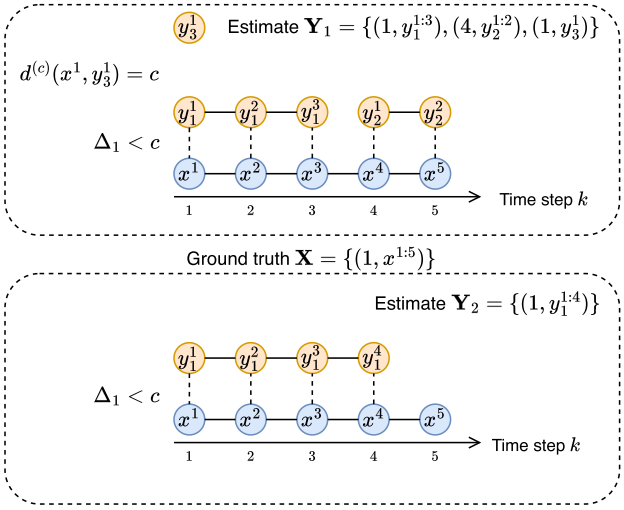

Fig. 2. Two estimated sets of trajectories $\mathbf{Y}_1$ and $\mathbf{Y}_2$ of the ground truth $\mathbf{X}$. The dashed lines represent assignments between the elements of the ground truth and the estimate. Estimate $\mathbf{Y}_1$ has five correct detections with localization error Δ_1, a false object, and a track switch. Estimate $\mathbf{Y}_2$ has four properly detected objects with localization error Δ_1 and a missed object.

D. Examples

We illustrate how the T-GOSPA q-metric works in two examples.

1) *Example 1:* We illustrate how the T-GOSPA q-metric works under DP3-DP5 for the example in Fig. 2. As before, we consider the case $p = 1$. For sufficiently small γ, estimate $\mathbf{Y}_1$ has five properly detected objects with localization error Δ_1, a false object, and a track switch, resulting in the value

$$d_1^{(c,\rho)}(\mathbf{X},\mathbf{Y}_1) = 5\Delta_1 + \rho c + \gamma. \tag{19}$$

It should be noted that if γ were sufficiently high, the optimal assignments are fixed across time, and therefore, the optimal assignment for $\mathbf{Y}_1$ would not be the one in Fig. 2. In this case, it would be optimal to leave the trajectory $(4, y_2^{1:2})$ unassigned with an overall q-metric value $3\Delta_1 + \rho c + 2c$. That is, we substitute the localization costs for two objects $(2\Delta_1)$ plus the track switching cost γ in (19) by the cost of two missed objects and two false objects $(2c)$, which would result in $\mathbf{Y}_2$ being always better than $\mathbf{Y}_1$, regardless of ρ.

Therefore, for sufficiently small γ, the optimal assignment is the one in Fig. 2 if

$$5\Delta_1 + \rho c + \gamma < 3\Delta_1 + \rho c + 2c \tag{20}$$

which implies that the track switching cost must meet

$$\gamma < 2(c - \Delta_1). \tag{21}$$

On the other hand, estimate $\mathbf{Y}_2$ has four properly detected objects with localization error Δ_1 and a missed object,

TABLE II
Distances/scores for the Example in Fig. 2 When Some Estimates are Close and When All of Them are Far Away

	Close		Far away	
	$\mathbf{Y}_1$	$\mathbf{Y}_2$	$\mathbf{Y}_1$	$\mathbf{Y}_2$
TGOSPA	$5\Delta_1 + \rho c + \gamma$	$4\Delta_1 + (1-\rho)\,c$	$(5+\rho)\,c$	$(5-\rho)\,c$
OSPA$^{(2)}$	$\frac{\Delta_1+4c}{5}$	$\frac{4\Delta_1+c}{5}$	c	c
UOSPA$^{(2)}$	$\frac{3\Delta_1+12c}{5}$	$\frac{4\Delta_1+c}{5}$	$3c$	c
HOTA(↑)	$\sqrt{\frac{13}{30}} \approx 0.66$	$\frac{4}{5} = 0.8$	0	0

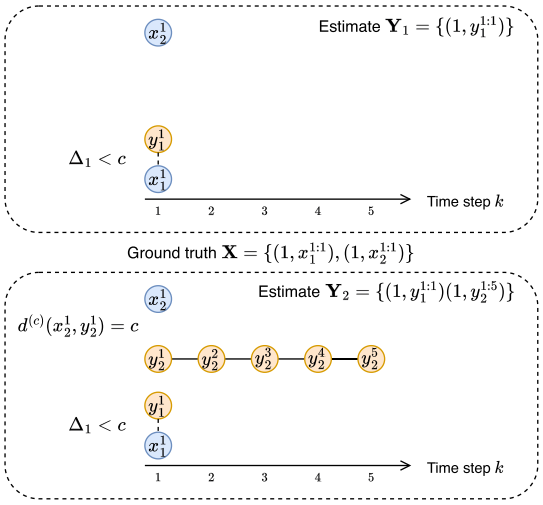

Fig. 3. Two estimated sets of trajectories $\mathbf{Y}_1$ and $\mathbf{Y}_2$ of the ground truth $\mathbf{X}$. The dashed lines represent assignments between the elements of the ground truth and the estimate. Estimate $\mathbf{Y}_1$ has five one correct detection with localization error Δ_1, and a missed object. Estimate $\mathbf{Y}_2$ has an additional false trajectory of length 5.

resulting in the value

$$d_1^{(c,\rho)}(\mathbf{X}, \mathbf{Y}_2) = 4\Delta_1 + (1-\rho)\,c. \tag{22}$$

According to the T-GOSPA q-metric, the estimate $\mathbf{Y}_2$ is more accurate than $\mathbf{Y}_1$ if

$$\rho > \frac{c - \Delta_1 - \gamma}{2c}. \tag{23}$$

The values of OSPA$^{(2)}$, UOSPA$^{(2)}$, and HOTA values are given in Table II ("Close estimates" column). The T-GOSPA metric ($\rho = 0.5$), OSPA$^{(2)}$, UOSPA$^{(2)}$, and HOTA indicate that $\mathbf{Y}_2$ is more accurate than $\mathbf{Y}_1$. However, setting ρ small enough (indicating a low cost for false objects), the T-GOSPA q-metric can determine that $\mathbf{Y}_1$ is more accurate. For instance, setting $c = 1$, $\Delta_1 = 0.1$, and $\gamma = 0.1$, $\mathbf{Y}_1$ is more accurate than $\mathbf{Y}_2$ if $\rho < 0.4$.

Let us now analyze the case where all estimates are far away ($\Delta_1 > c$) in Fig. 3. In this case, $\mathbf{Y}_1$ has five missed objects and six false objects, while $\mathbf{Y}_2$ has five missed objects and four false objects. T-GOSPA and UOSPA$^{(2)}$ indicate that $\mathbf{Y}_2$ is more accurate, meeting DP4. On the contrary, OSPA$^{(2)}$ and HOTA indicate that both estimates are equally accurate.

2) *Example 2:* We now consider the example in Fig. 3, in which estimate $\mathbf{Y}_2$ has an extra false trajectory of length 5 compared to $\mathbf{Y}_1$. The errors are shown in Table III. OSPA$^{(2)}$ and UOSPA$^{(2)}$ do not penalize this extra false trajectory (which could be arbitrarily long) and indicate that $\mathbf{Y}_1$ and $\mathbf{Y}_2$ are equally accurate. HOTA and T-GOSPA work according to DP4. If all estimates are far away, then only T-GOSPA indicates that $\mathbf{Y}_1$ is more accurate than $\mathbf{Y}_2$, as expected according to DP4.

TABLE III
Distances/scores for the Example in Fig. 3 When Some Estimates are Close and When All of Them are Far Away

	Close		Far away	
	$\mathbf{Y}_1$	$\mathbf{Y}_2$	$\mathbf{Y}_1$	$\mathbf{Y}_2$
TGOSPA	$\Delta_1 + (1-\rho)\,c$	$\Delta_1 + (1+4\rho)\,c$	$(2-\rho)\,c$	$(2+4\rho)\,c$
OSPA$^{(2)}$	$\frac{\Delta_1+c}{2}$	$\frac{\Delta_1+c}{2}$	c	c
UOSPA$^{(2)}$	$\Delta_1 + c$	$\Delta_1 + c$	$2c$	$2c$
HOTA(↑)	$\frac{1}{\sqrt{2}}$	$\frac{1}{\sqrt{7}}$	0	0

E. Properties

This section extends the properties of the GOSPA q-metric presented in Section III-D to the T-GOSPA q-metric. The following result holds directly from the definition.

LEMMA 9 If $d_b(\cdot,\cdot)$ is a metric, then the T-GOSPA q-metric and its LP relaxation meet

$$d_p^{(c,\rho,\gamma)}(\mathbf{X}, \mathbf{Y}) = d_p^{(c,1-\rho,\gamma)}(\mathbf{Y}, \mathbf{X}) \tag{24}$$

$$\overline{d}_p^{(c,\rho,\gamma)}(\mathbf{X}, \mathbf{Y}) = \overline{d}_p^{(c,1-\rho,\gamma)}(\mathbf{Y}, \mathbf{X}). \tag{25}$$

The following lemma regarding the optimal assignment is proved in Appendix E-A of the Supplementary Material.

LEMMA 10 The optimal sequence of matrices $W^k \in \overline{\mathcal{W}}_{\mathbf{X},\mathbf{Y}}$ with $k = 1, \ldots, T$ in the LP T-GOSPA q-metric does not depend on ρ. Similarly, the optimal sequence of matrices $W^k \in \mathcal{W}_{\mathbf{X},\mathbf{Y}}$ with $k = 1, \ldots, T$ in the T-GOSPA q-metric does not depend on ρ.

A direct consequence of this lemma is that the optimal sequence of assignment vectors $\pi^k \in \Pi_{\mathbf{X},\mathbf{Y}}$, $k = 1, \ldots, T$ of the T-GOSPA q-metric does not depend on ρ. Lemma 10 implies that for different values of ρ, the localization and track switching costs remain unchanged, but there are different missed and false object costs. In addition, this implies that if $d_b(\cdot,\cdot)$ is a metric, then the optimal W^k is the same as in the T-GOSPA metric. If we want to compute the q-metric for several values of ρ, then this lemma provides a computational advantage, as it suffices to solve the optimization problem once.

The T-GOSPA q-metric symmetrization property is provided in the following lemma, and proved in Appendix E-B of the Supplementary Material.

LEMMA 11 If $d_b(\cdot,\cdot)$ is a metric, then the T-GOSPA metrics $d_p^{(c,1/2,\gamma)}(\mathbf{X}, \mathbf{Y})$ and $\overline{d}_p^{(c,1/2,\gamma)}(\mathbf{X}, \mathbf{Y})$ are recovered with the following symmetrization of the TGOSPA q-metrics:

$$d_p^{(c,1/2,\gamma)}(\mathbf{X}, \mathbf{Y}) = \left[\frac{1}{2}\left(d_p^{(c,\rho,\gamma)}(\mathbf{X}, \mathbf{Y})^p + d_p^{(c,\rho,\gamma)}(\mathbf{Y}, \mathbf{X})^p\right)\right]^{1/p} \tag{26}$$

$$\overline{d}_p^{(c,1/2,\gamma)}(\mathbf{X},\mathbf{Y}) = \left[\frac{1}{2}\left(\overline{d}_p^{(c,\rho,\gamma)}(\mathbf{X},\mathbf{Y})^p + \overline{d}_p^{(c,\rho,\gamma)}(\mathbf{Y},\mathbf{X})^p\right)\right]^{1/p}. \quad (27)$$

V. Q-METRIC-BASED SIMILARITY SCORE FUNCTIONS

In this section, we present the definition of q-metric-based scores in Section V-A. Then, in Section V-B, we provide examples of metric-preserving mappings, which are required to define the q-metric-based scores. Section V-C defines the q-metric-based scores based on GOSPA and T-GOSPA.

A. Q-Metric-Based Score Definition

We define a q-metric-based score function on a given space Υ, to measure the similarity between $\mathbf{X}, \mathbf{Y} \in \Upsilon$, as a function $s(\cdot,\cdot) : \Upsilon \times \Upsilon \to [0,1]$ that meets the following properties.

1) $s(\mathbf{X},\mathbf{Y}) = 1$ if and only if $\mathbf{X} = \mathbf{Y}$.
2) $s(\mathbf{X},\mathbf{Y}) + 1 \geq s(\mathbf{X},\mathbf{Z}) + s(\mathbf{Z},\mathbf{Y})$.

If, additionally, $s(\mathbf{X},\mathbf{Y}) = s(\mathbf{Y},\mathbf{X})$, then we say that $s(\cdot,\cdot)$ is a metric-based score. Clearly, $s(\cdot,\cdot)$ is a q-metric-based score if and only if $1 - s(\cdot,\cdot)$ is a q-metric. These properties define score functions based on mathematically principled notions of error (given by metrics or q-metrics). We consider two cases to obtain q-metric-based scores, the first one is for bounded q-metrics and the second one is for unbounded q-metrics.

Let us consider that $d(\cdot,\cdot)$ is a bounded q-metric (for instance, the OSPA metric [7], [8]), whose image supremum is c. Then, a q-metric-based score is simply obtained as $1 - d(\cdot,\cdot)/c$. Now, let us proceed to build score functions for unbounded q-metrics (such as the ones proposed in this article, UOSPA, or COLA) using metric-preserving mappings [40].

We first consider a function $f(\cdot) : [0,\infty) \to [0,1]$ with the following properties.

1) *P1:* $f^{-1}(0) = \{0\}$.
2) *P2:* $f(\cdot)$ is nondecreasing.
3) *P3:* $f(\cdot)$ is subadditive, meaning that [41, Ch. VII], for $a \geq 0$ and $b \geq 0$
$$f(a+b) \leq f(a) + f(b). \quad (28)$$
4) *P4:* $\lim_{x\to\infty} f(x) = 1$.

P1–P3 implies that $f(\cdot)$ is a metric-preserving mapping, and P4 is required to build a score function.

LEMMA 12 Given a function $f(\cdot)$ that meets P1–P4 and a q-metric $d(\cdot,\cdot)$ on a space Υ, their composition, $f(d(\cdot,\cdot))$, is a q-metric on space Υ taking values in $[0,1]$. This implies that $s(\cdot,\cdot) = 1 - f(d(\cdot,\cdot))$ is a q-metric-based similarity score function.

For completeness, the proof of Lemma 12 is provided in Appendix F of the Supplementary Material. It should be noted that P1–P3 imply that $f(\cdot)$ is a metric-preserving mapping [40] and are required to keep the q-metric properties. P4 is required such that the composed q-metric is bounded with supremum equal to 1, and therefore, $1 - f(d(\cdot,\cdot))$ is a q-metric-based score.

B. Examples of Metric-Preserving Mappings

This section provides some examples of functions that meet P1–P4 and define q-metric-based scores for unbounded q-metrics. We include a positive parameter $\beta > 0$ to the mappings to give more flexibility to the design of the score. The mappings are the scaled and translated sigmoid, the hyperbolic tangent function, the scaled arctangent function, and a fractional linear function, which are given in the following:

$$f_\beta(x) = 2\frac{1}{1+e^{-x/\beta}} - 1 \quad (29)$$
$$f_\beta(x) = \tanh(x/\beta) \quad (30)$$
$$f_\beta(x) = \frac{2}{\pi}\arctan(x/\beta) \quad (31)$$
$$f_\beta(x) = \frac{x/\beta}{1+x/\beta}. \quad (32)$$

These functions achieve keep the metric properties and map unbounded metric values to the interval $[0,1]$, with slightly different ways to perform the mapping.

C. Application to GOSPA and T-GOSPA Q-Metrics

Applying Lemma 12 and the metric-preserving mappings (29)–(32) to the GOSPA and T-GOSPA q-metrics, we obtain bounded versions of GOSPA and T-GOSPA q-metrics. If $f_\beta(\cdot)$ is an increasing function (which meets P2), then the bounded versions also meet the DPs DP1–DP3 or DP3–DP5, with the decomposition applying before the mapping $f_\beta(\cdot)$. In this case, we can see that while an increase of false objects is always penalized, each additional false object is penalized less. In addition, given sets $\mathbf{X}$, $\mathbf{Y}$, and $\mathbf{Z}$, if

$$d_p^{(c,\rho,\gamma)}(\mathbf{X},\mathbf{Y}) < d_p^{(c,\rho,\gamma)}(\mathbf{X},\mathbf{Z}) \quad (33)$$

then

$$f_\beta\left(d_p^{(c,\rho,\gamma)}(\mathbf{X},\mathbf{Y})\right) < f_\beta\left(d_p^{(c,\rho,\gamma)}(\mathbf{X},\mathbf{Z})\right) \quad (34)$$
$$1 - f_\beta\left(d_p^{(c,\rho,\gamma)}(\mathbf{X},\mathbf{Y})\right) > 1 - f_\beta\left(d_p^{(c,\rho,\gamma)}(\mathbf{X},\mathbf{Z})\right). \quad (35)$$

That is, for an increasing mapping $f_\beta(\cdot)$, the ranking of the estimates does not change, either with the bounded q-metric or with its associated score. As the GOSPA and T-GOSPA q-metrics have the units of the base distance $d_b(\cdot,\cdot)$, β must have the same units such that the units are removed for the mappings (29)–(32) to be well defined. In addition, parameter β can be set to calibrate the similarity in the score function. For example, we can fix β such that an estimate with n_{fa} false objects when the ground truth has no objects has a similarity score of $s_{n_{\text{fa}}}$. As the GOSPA q-metric error

in this case is $c\sqrt[p]{\rho n_{\text{fa}}}$, we can obtain β by solving

$$1 - f_\beta\left(c\sqrt[p]{\rho n_{\text{fa}}}\right) = s_{n_{\text{fa}}}. \tag{36}$$

EXAMPLE 13: Assume that in a given MOT system, there is a maximum localization error of $c = 10$ m. We use the GOSPA q-metric with $\rho = 0.5$ and $p = 1$. We design the similarity score with the sigmoid metric-preserving mapping (29) by setting the estimate with ten false objects, when there are no real objects, a score of 0.1. Calibrating the score function with (36) yields $\beta = 16.98$ m.

VI. Q-METRICS AND SCORES FOR RFSS

This section extends the GOSPA and T-GOSPA q-metrics, and their associated scores, to RFSs of objects [35] and trajectories [36]. This extension is relevant for performance evaluation via Monte Carlo simulations. It is also relevant for performance evaluation using a dataset containing multiple scenarios, each associated with a different ground truth. It is possible to understand these two cases as the comparison between an RFS with the ground truth and another RFS with the estimate [22, Sect. V].

A. Q-Metrics

The GOSPA q-metric can be extended to RFSs of objects using the expected GOSPA q-metric value, as done for the GOSPA metric [14, Sect. III]. We consider a real parameter p' such that $1 \leq p' < \infty$. The expected value of the GOSPA q-metric to the p' power is

$$\mathbb{E}\left[d_p^{(c,\rho)}(\mathbf{x},\mathbf{y})^{p'}\right] = \int\int d_p^{(c,\rho)}(\mathbf{x},\mathbf{y})^{p'}\, p(\mathbf{x},\mathbf{y})\, \delta\mathbf{x}\delta\mathbf{y} \tag{37}$$

where this expectation is a double set integral [35] taken with respect to the joint density $p(\mathbf{x}, \mathbf{y})$ of the RFSs $\mathbf{x}$ and $\mathbf{y}$.

Similarly, we can extend the T-GOSPA q-metric to RFSs of trajectories using the expected T-GOSPA q-metric value. The expected value of the T-GOSPA q-metric to the p' power has the same expression as (37), but using $\mathbf{X}$ and $\mathbf{Y}$ instead of $\mathbf{x}$ and $\mathbf{y}$, and sets integrals for sets of trajectories [36] instead of sets integrals for sets of objects. Then, we have this result.

LEMMA 14 For a real parameter p' such that $1 \leq p' < \infty$, $(\mathbb{E}[d_p^{(c,\rho)}(\mathbf{x},\mathbf{y})^{p'}])^{1/p'}$ is a q-metric on the space of RFSs of objects with a finite cardinality moment $\mathbb{E}[|\cdot|^{p'/p}] < \infty$. In addition, $(\mathbb{E}[d_p^{(c,\rho,\gamma)}(\mathbf{X},\mathbf{Y})^{p'}])^{1/p'}$ and $(\mathbb{E}[\overline{d}_p^{(c,\rho,\gamma)}(\mathbf{X},\mathbf{Y})^{p'}])^{1/p'}$ are q-metrics on the space of RFSs of trajectories with a finite cardinality moment $\mathbb{E}[|\cdot|^{p'/p}] < \infty$.

The proof is equivalent to the proof of [24, Lemma 3].

B. Q-Metric-Based Scores

The extension of the q-metric-based scores to RFSs of objects and trajectories is provided via the following lemma.

LEMMA 15 Given the GOSPA and T-GOSPA q-metric scores $s(\mathbf{x},\mathbf{y}) = 1 - f_\beta(d_p^{(c,\rho)}(\mathbf{x},\mathbf{y}))$ and $s(\mathbf{X},\mathbf{Y}) = 1 - f_\beta(d_p^{(c,\rho,\gamma)}(\mathbf{X},\mathbf{Y}))$, $\mathbb{E}[s(\mathbf{x},\mathbf{y})]$ and $\mathbb{E}[s(\mathbf{X},\mathbf{Y})]$ are q-metric-based scores on the space of RFSs of objects and RFSs of trajectories, respectively.

The proof is similar to the one of Lemma 14 considering $p' = 1$. When we deal with scores and RFSs, we simply take the expected value to keep the q-metric-based score property. In simulation-based MOT evaluation, the expected values in Lemmas 14 and 15 are approximated via Monte Carlo simulation, as done in the next section.

VII. SIMULATIONS

This section examines the performance of several Bayesian MOT algorithms via the T-GOSPA q-metric, OSPA$^{(2)}$, and UOSPA$^{(2)}$. We have implemented the trajectory Poisson multi-Bernoulli mixture (T-PMBM) filter [42], the PMBM filter [43], [44], and the generalized labeled multi-Bernoulli (GLMB) filter.[3] The PMBM and GLMB both use sequential track formation by connecting state estimates with a similar auxiliary variable, track index (PMBM) [46] or with the same label (GLMB). T-PMBM and PMBM consider a maximum number of 200 global hypotheses, while GLMB has a maximum of 1000. All filters use Murty's algorithm [47] in the update step to select the global hypotheses, arising from a previous global hypotheses, that have the highest weights. The T-PMBM implementation uses an L-scan window with $L = 5$, to jointly update the last L time steps of single-trajectory densities. The pruning and estimation parameters are set as in [46]. All units are in the international system and are not included for brevity.

The state of a single object is $x = [p_x, \dot{p}_x, p_y, \dot{p}_y]^T$, containing 2-D position $[p_x, p_y]^T$ and velocity $[\dot{p}_x, \dot{p}_y]^T$. Objects move with a nearly constant velocity model [48] with a sampling time $\tau = 1$, and the process noise intensity is $q = 0.4$. The probability of survival of the objects is 0.99.

The birth single-object density is $p_b(x) = \mathcal{N}(x; \bar{x}_b, P_b)$, which represents a Gaussian density with mean $\bar{x}_b = [400, 0, 400, 0]^T$ and covariance matrix $P_b = \text{diag}([300^2, 2^2, 300^2, 2^2])$. For T-PMBM and PMBM filters, the birth model is a Poisson point process (PPP). Its intensity is $3p_b(x)$ at the initial time step ($k = 1$) and $0.005p_b(x)$ at the following time steps. The GLMB filter uses a multi-Bernoulli birth model, which is chosen to approximate the PPP birth model with five Bernoulli components as in [46].

The probability of detection of each object is set to $p^D = 0.9$. The sensor measures the positional elements with an additive zero-mean Gaussian noise with covariance matrix $R = \text{diag}([4, 4])$. Clutter follows a PPP whose intensity is $\lambda^C(z) = \overline{\lambda}^C u_A(z)$ where $\overline{\lambda}^C = 20$ and $u_A(z)$ is a uniform density in the area $A = [0, 800] \times [0, 800]$. The simulation has 101 time steps and contains four objects. The scenario

[3]Code of the T-PMBM and PMBM filters can be found at https://github.com/Agarciafernandez/MTT. Code of the GLMB filter can be found at https://ba-tuong.vo-au.com. [45]

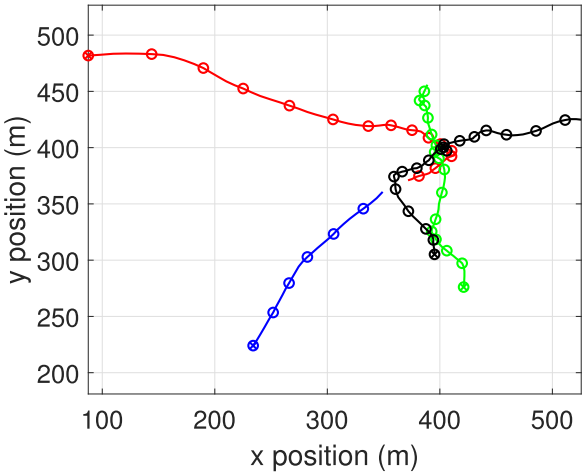

Fig. 4. Scenario considered the simulations. All objects appear at time step 1 except the black one, which appears at time step 6. The initial object states are marked with a cross. The blue object dies at time step 30, the red at time step 75, the green at time step 80 and the black one at time step 100.

is represented in Fig. 4. Three of these objects get in close proximity roughly at the middle of the simulation[4].

At each time step, we evaluate the accuracy of the estimated set $\hat{\mathbf{X}}_k$ of all trajectories (positional elements) up to the current time step k compared with the true set $\mathbf{X}_k$ of all trajectories via Monte Carlo simulation with $N_{\text{mc}} = 100$ runs. The T-GOSPA q-metric has been implemented with the Euclidean distance, parameter $p = 2$, maximum localization error $c = 10$, track switching penalty $\gamma = 1$, and q-metric parameter $\rho \in \{0.3, 0.5, 0.7\}$. We consider three choices of ρ to analyze the effect of this parameter in the q-metric value. With $\rho = 0.3$, missed objects are penalized more than false objects. With $\rho = 0.5$, missed and false objects are penalized equally (T-GOSPA metric). With $\rho = 0.7$, false objects are penalized more than missed objects. The root mean square (RMS) T-GOSPA q-metric at time step k is

$$d(k) = \sqrt{\frac{1}{N_{\text{mc}} k} \sum_{i=1}^{N_{\text{mc}}} d_2^{(10,\rho,1)} \left(\mathbf{X}_k, \hat{\mathbf{X}}_k^i\right)^2} \qquad (38)$$

where the squared q-metric has been normalized by the time window length k (the time window is from time step 1 to k). Equation (38) is a Monte Carlo approximation of the q-metric for RFSs in Lemma 14. In this case, $\mathbf{X}_k$ can be considered a deterministic RFS, and $\hat{\mathbf{X}}_k^i$ are realizations of the estimated RFS of trajectories. The T-GOSPA similarity score has been implemented with the scaled and translated sigmoid (29). To account for the increasing window length, the β parameter of the score is chosen as $\beta = k\beta_0$, where β_0 is chosen using (36) to return a score of 0.1 with 50 false targets and $\rho = 0.5$, resulting in $\beta_0 = 16.98$. OSPA$^{(2)}$ and

[4]Code with the scenario to reproduce the results is available at https://github.com/Agarciafernandez/MTT.

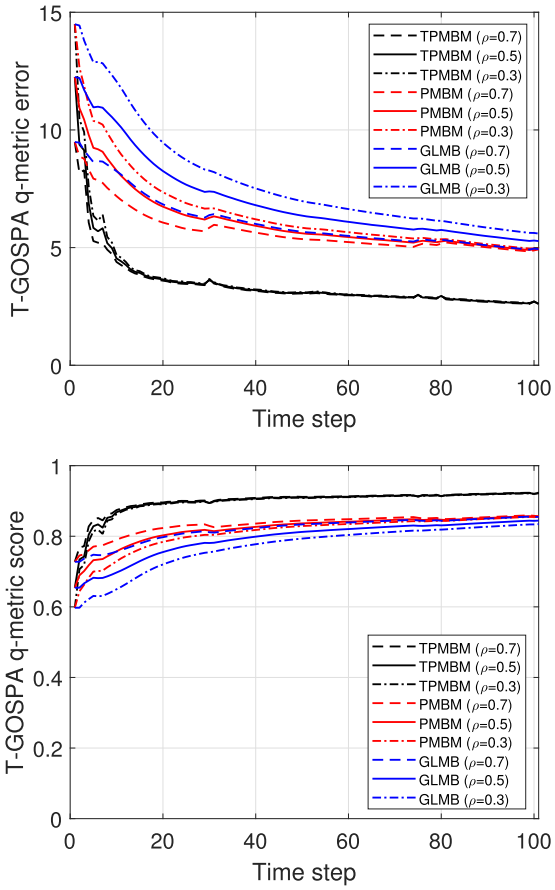

Fig. 5. RMS-T-GOSPA q-metric errors at each time step (top) and mean T-GOSPA q-metric scores at each time step (bottom). The TPMBM filter performs best for all considered values of ρ.

UOSPA$^{(2)}$ also use $p = 2$ and $c = 10$, and their RMS errors are computed similarly to (38).

We first analyze the effect of parameter ρ. The RMS-T-GOSPA q-metric errors and the mean T-GOSPA scores at each time step are shown in Fig. 5. We can see that the ranking of the algorithms remains unchanged either looking at the errors or the scores. For all choices of ρ, the T-PMBM filter achieves the best performance, followed by PMBM and then GLMB. The q-metric errors are higher with $\rho = 0.3$ than with the other values of ρ. This means that in this scenario there are more missed objects than false objects, which can also be checked in the error decomposition in Fig. 6. Overall, the q-metric value decreases with time since the estimation of all the trajectories becomes more accurate (normalized by the time window length). While localization errors stay roughly the same across time, the missed object cost decreases since objects are mainly missed at the beginning of the simulation, so their normalized cost decreases with time. At the time steps when some objects disappear, there are some spikes in the T-GOSPA error, due to false alarms. We can see that the spikes are larger with $\rho = 0.7$ since higher ρ penalizes false objects more. From Lemma 10, we know that the localization error and track switching cost do not change with ρ. This can be seen in Fig. 6.

TABLE IV
RMS-TGOSPA Q-Metric Errors Across All Time Steps

p^D	$\overline{\lambda}^C$	T-PMBM $\rho=$ 0.3	0.5	0.7	PMBM $\rho=$ 0.3	0.5	0.7	PMB $\rho=$ 0.3	0.5	0.7	GLMB $\rho=$ 0.3	0.5	0.7
0.7	15	5.69	5.47	5.25	8.37	7.71	7.00	8.35	7.81	7.23	9.68	8.61	7.39
	20	5.72	5.47	5.21	8.43	7.77	7.04	8.42	7.88	7.29	9.88	8.76	7.47
	25	6.08	5.73	5.36	8.72	7.96	7.12	8.67	8.07	7.42	10.17	8.98	7.61
0.8	15	4.57	4.28	3.98	7.46	6.89	6.26	7.43	6.95	6.43	8.83	7.85	6.73
	20	4.79	4.50	4.18	7.64	7.03	6.36	7.61	7.10	6.55	9.13	8.09	6.90
	25	5.26	4.82	4.34	7.98	7.29	6.52	7.83	7.27	6.66	9.38	8.29	7.04
0.9	15	3.97	3.78	3.58	6.75	6.29	5.80	6.70	6.29	5.85	8.16	7.25	6.21
	20	4.08	3.84	3.59	6.84	6.34	5.80	6.78	6.34	5.86	8.35	7.39	6.29
	25	4.23	3.94	3.62	7.07	6.52	5.91	6.95	6.47	5.96	8.57	7.57	6.42
0.95	15	3.70	3.51	3.30	6.40	5.91	5.37	6.37	5.92	5.43	7.83	6.95	5.94
	20	3.70	3.51	3.32	6.43	5.93	5.38	6.40	5.95	5.46	7.98	7.06	6.00
	25	3.88	3.66	3.42	6.62	6.08	5.52	6.54	6.07	5.56	8.18	7.22	6.12

TABLE V
RMS-OSPA$^{(2)}$ and RMS-UOSPA$^{(2)}$ Metric Errors Across All Time Steps

p^D	$\overline{\lambda}^C$	T-PMBM OSPA$^{(2)}$	T-PMBM UOSPA$^{(2)}$	PMBM OSPA$^{(2)}$	PMBM UOSPA$^{(2)}$	PMB OSPA$^{(2)}$	PMB UOSPA$^{(2)}$	GLMB OSPA$^{(2)}$	GLMB UOSPA$^{(2)}$
0.7	15	4.20	8.23	6.28	13.56	6.41	14.19	7.23	15.83
	20	4.35	8.64	6.52	14.46	6.58	14.90	7.29	15.87
	25	4.44	8.74	6.64	14.58	6.77	15.31	7.43	16.04
0.8	15	3.46	6.74	5.68	12.08	5.71	12.22	6.71	14.44
	20	3.69	7.29	5.98	12.96	6.01	13.13	6.93	15.04
	25	3.84	7.51	6.18	13.43	6.20	13.88	6.98	14.98
0.9	15	3.23	6.36	5.45	11.73	5.45	11.68	6.16	12.97
	20	3.51	7.04	5.51	11.95	5.45	11.90	6.14	12.69
	25	3.26	6.42	5.54	11.85	5.70	12.48	6.31	13.18
0.95	15	3.00	5.87	4.77	9.73	4.88	10.01	5.97	12.42
	20	3.09	6.17	5.01	10.57	5.17	10.98	5.96	12.40
	25	3.13	6.14	5.30	11.31	5.32	11.40	6.10	12.65

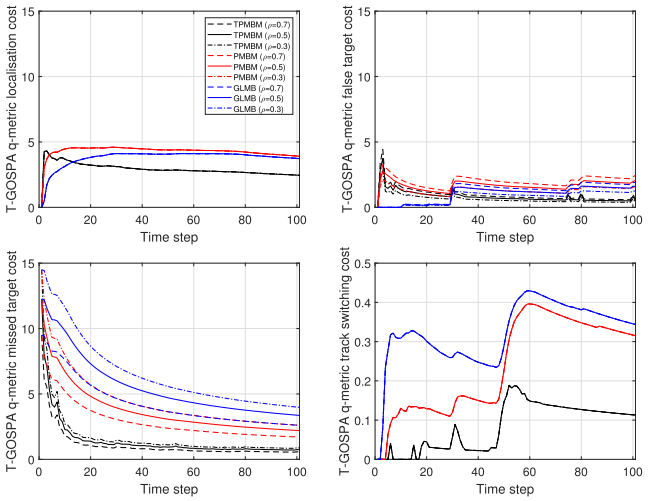

Fig. 6. RMS-T-GOSPA q-metric decomposition across time. A change in ρ implies a change in the false and missed object costs, whereas localization and track switching costs remain unchanged. Thus, there is only one line style visible for each filter in the first and last subfigures.

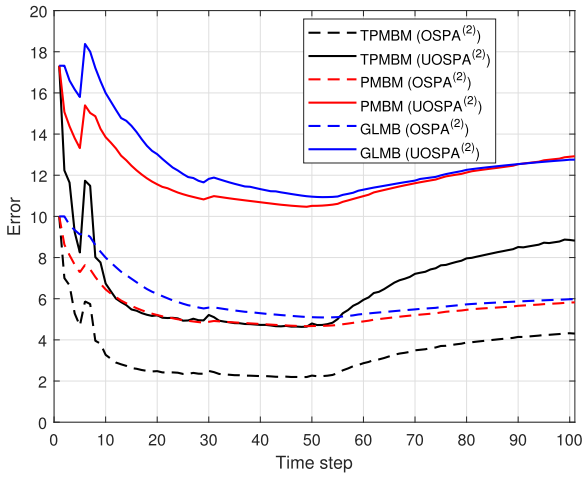

Fig. 7. RMS-OSPA$^{(2)}$ and RMS-UOSPA$^{(2)}$ errors at each time step. The TPMBM filter performs the best.

The RMS-OSPA$^{(2)}$ and RMS-UOSPA$^{(2)}$ errors at each time step are shown in Fig. 7. In this case, these metrics agree with the ranking of algorithms provided by the T-GOSPA q-metric. While we can decompose this plot into cardinality errors and another error for trajectory mismatch, it is not possible to decompose the error as in Fig. 6, not meeting DP5.

We now proceed to evaluate tracking performance for different values of p^D and $\overline{\lambda}^C$. The RMS-GOSPA error across all time steps is shown in Table IV. As space allows, this table also includes the (track-oriented) PMB filter [43] with sequential track building. The best performing filter is always the T-PMBM filter, followed by PMBM/PMB (depending on the scenario) and then followed by GLMB. As expected, higher clutter and lower p^D generally increase the error (this happens in all entries except for the T-PMBM $\rho = 0.7$ and $\overline{\lambda}^C = 20$). In the considered scenarios, the missed object error dominates the false object error since q-metric value is the highest for $\rho = 0.3$. The RMS-OSPA$^{(2)}$ and RMS-UOSPA$^{(2)}$ errors across all time steps are shown

in Table V. In these results, we can see that increasing the clutter rate does not increase the metric value as consistently as with T-GOSPA q-metric (entries highlighted in red). In these cases, these metrics are indicating that the results with higher clutter rate are preferable with those with a smaller clutter rate. A factor that is contributing to these results for these metrics is that assignments of real to estimated trajectories cannot change over time. All metrics and q-metrics indicate that all algorithms with $\overline{\lambda}^{C} = 15$ perform better than the same algorithms with $\overline{\lambda}^{C} = 25$, as expected.

VIII. CONCLUSION

This article has presented two quasi-metrics for performance evaluation of MOT algorithms, with the important characteristic of being clearly interpretable to penalize localization errors, the number of missed and false objects, and track switches. This interpretability enables a fair comparison of the estimated sets of objects or sets of trajectories provided by different algorithms since these q-metrics promote algorithms with lower values of the indicated errors. The proposed quasi-metrics are extensions of the GOSPA metrics for sets of objects, and sets of trajectories, and allow uneven costs for the missed and false objects. This article proves the identity and triangle inequality properties that are required to define quasi-metrics. The article has also presented how to define similarity score functions based on the GOSPA and T-GOSPA quasi-metrics. The proposed quasi-metrics and their scores have also been extended to RFSs of objects and RFSs of trajectories.

The T-GOSPA q-metric has been applied to evaluate MOT simulation results for different values of ρ, showing the effects on the q-metric value of using different costs for missed and false objects. The GOSPA and T-GOSPA quasi-metrics should be used in applications in which the user is interested in penalizing missed and false objects differently, according to DPs DP1–DP5. This can be achieved by choosing the parameter ρ accordingly. In other cases, our recommendation for evaluation of MOT algorithms is to use the GOSPA and T-GOSPA metrics as well as their decompositions into their different components to provide a more thorough analysis. It is also true that there can be applications in which users prefer metrics with different DPs from DP1–DP5, for instance, metrics that penalize cardinality mismatch instead of the number of missed and false objects. In these cases, it can be reasonable to use other metric, for instance, OSPA, UOSPA, COLA, or GOSPA ($\alpha \neq 2$).

A direction of future work is to extend the proposed quasi-metrics to uncertainty-aware MOT performance evaluation, as done for GOSPA and T-GOSPA in [49] and [50]. Another direction of future work is the application of these quasi-metrics to computer vision MOT performance evaluation. In addition, future work can develop of other quasi-metrics for MOT performance evaluation, instead of the standard (symmetric) metrics.

REFERENCES

[1] D. M. Jiménez-Bravo et al., "Multi-object tracking in traffic environments: A systematic literature review," *Neurocomputing*, vol. 494, pp. 43–55, 2022.

[2] P. Braca, P. Willett, K. LePage, S. Marano, and V. Matta, "Bayesian tracking in underwater wireless sensor networks with port-starboard ambiguity," *IEEE Trans. Signal Process.*, vol. 62, no. 7, pp. 1864–1878, Apr. 2014.

[3] E. Delande, J. Houssineau, J. Franco, C. Frueh, D. Clark, and M. Jah, "A new multi-target tracking algorithm for a large number of orbiting objects," *Adv. Space Res.*, vol. 64, pp. 645–667, 2019.

[4] S. Blackman and R. Popoli, *Design and Analysis of Modern Tracking Systems*. Norwood, MA, USA: Artech House, 1999.

[5] K. Smith, D. Gatica-Perez, J. Odobez, and S. Ba, "Evaluating multi-object tracking," in *Proc. IEEE Comput. Soc. Conf. Comput. Vis. Pattern Recognit.*, 2005, pp. 36–36.

[6] T. M. Apostol, *Mathematical Analysis*. Boston, MA, USA: Addison Wesley, 1974.

[7] D. Schuhmacher and A. Xia, "A new metric between distributions of point processes," *Adv. Appl. Probability*, vol. 40, no. 3, pp. 651–672, Sep. 2008.

[8] D. Schuhmacher, B.-T. Vo, and B.-N. Vo, "A consistent metric for performance evaluation of multi-object filters," *IEEE Trans. Signal Process.*, vol. 56, no. 8, pp. 3447–3457, Aug. 2008.

[9] P. Barrios, M. Adams, K. Leung, F. Inostroza, G. Naqvi, and M. E. Orchard, "Metrics for evaluating feature-based mapping performance," *IEEE Trans. Robot.*, vol. 33, no. 1, pp. 198–213, Feb. 2017.

[10] P. Barrios and M. Adams, "A comparison of multi-object sub-pattern linear assignment metrics," in *Proc. 12th Int. Conf. Control, Automat. Inf. Sci.*, 2023, pp. 712–718.

[11] J. L. Williams, "An efficient, variational approximation of the best fitting multi-Bernoulli filter," *IEEE Trans. Signal Process.*, vol. 63, no. 1, pp. 258–273, Jan. 2015.

[12] J. R. Hoffman and R. P. S. Mahler, "Multitarget miss distance via optimal assignment," *IEEE Trans. Syst., Man, Cybern. - Part A: Syst. Humans*, vol. 34, no. 3, pp. 327–336, May 2004.

[13] T. Vu, "A complete optimal subpattern assignment (COSPA) metric," in *Proc. 23rd Int. Conf. Inf. Fusion*, 2020, pp. 1–8.

[14] A. S. Rahmathullah, A. F. García-Fernández, and L. Svensson, "Generalized optimal sub-pattern assignment metric," in *Proc. 20th Int. Conf. Inf. Fusion*, 2017, pp. 1–8.

[15] H. Suljagic, E. Bayraktar, and N. Celebi, "Similarity based person re-identification for multi-object tracking using deep Siamese network," *Neural Comput. Appl.*, vol. 34, pp. 18171–18182, 2022.

[16] E. Bayraktar, Y. Wang, and A. DelBue, "Fast re-OBJ: Real-time object re-identification in rigid scenes," *Mach. Vis. Appl.*, vol. 33, pp. 1–12, 2022.

[17] E. Bayraktar, "ReTrackVLM: Transformer-enhanced multi-object tracking with cross-modal embeddings and zero-shot re-identification integration," *Appl. Sci.*, vol. 15, no. 4, 2025, Art. no. 1907.

[18] K. Bernardin and R. Stiefelhagen, "Evaluating multiple object tracking performance: The CLEAR MOT metrics," *EURASIP J. Image Video Process.*, vol. 2008, 2008, Art. no. 246309.

[19] H. Caesar et al., "nuScenes: A multimodal dataset for autonomous driving," in *Proc. IEEE/CVF Conf. Comput. Vis. Pattern Recognit.*, 2020, pp. 11618–11628.

[20] J. Luiten et al., "HOTA: A higher order metric for evaluating multi-object tracking," *Int. J. Comput. Vis.*, vol. 129, pp. 548–578, 2020.

[21] M. Beard, B. T. Vo, and B. Vo, "A solution for large-scale multi-object tracking," *IEEE Trans. Signal Process.*, vol. 68, pp. 2754–2769, 2020.

[22] A. F. García-Fernández, A. S. Rahmathullah, and L. Svensson, "A time-weighted metric for sets of trajectories to assess multi-object tracking algorithms," in *Proc. 24th Int. Conf. Inf. Fusion*, 2021, pp. 1–8.

[23] J. Bento and J. J. Zhu, "A metric for sets of trajectories that is practical and mathematically consistent," 2018, *arXiv:1601.03094*.
[24] A. F. García-Fernández, A. S. Rahmathullah, and L. Svensson, "A metric on the space of finite sets of trajectories for evaluation of multi-target tracking algorithms," *IEEE Trans. Signal Process.*, vol. 68, pp. 3917–3928, 2020.
[25] V. N. Wernholm, A. Wärnsäter, and A. Ringh, "Fast computation of the TGOSPA metric for multiple target tracking via unbalanced optimal transport," *IEEE Contr. Syst. Lett.*, vol. 9, pp. 498–503, 2025.
[26] A. Wärnsäter, Y. Xia, T. Yuan, and J. Karlsson, "Efficient approximation of the trajectory GOSPA metric via graph-structured optimal transport," in *Proc. IEEE Radar Conf.*, 2025, pp. 443–448.
[27] M. Skolnik, *Introduction to Radar Systems*. Columbus, OH, USA: McGraw-Hill, 2001.
[28] W. A. Wilson, "On quasi-metric spaces," *Amer. J. Math.*, vol. 53, no. 3, pp. 675–684, Jul. 1931.
[29] V. Schroeder, "Quasi-metric and metric spaces," *Conformal Geometry Dyn.*, vol. 10, pp. 355–360, Dec. 2006.
[30] J. Bento and S. Ioannidis, "A family of tractable graph metrics," *Appl. Netw. Sci.*, vol. 4, 2019, Art. no. 107.
[31] A. Stojmirović, "Quasi-metrics, similarities and searches: Aspects of geometry of protein datasets," Ph.D. dissertation, Victoria Univ. Wellington, 2005.
[32] T. Wang, A. Torralba, P. Isola, and A. Zhang, "Optimal goal-reaching reinforcement learning via quasimetric learning," in *Proc. 40th Int. Conf. Mach. Learn.*, 2023, pp. 36411–36430.
[33] T. Wang and P. Isola, "On the learning and learnability of quasimetrics," in *Proc. Int. Conf. Learn. Representations*, 2022, pp. 1–14.
[34] T. Li, Y. Song, H. Fan, and J. Chen, "From target tracking to targeting track - Part I: A metric for spatio-temporal trajectory evaluation," *Inf. Fusion*, vol. 127, 2026, Art. no. 103890.
[35] R. P. S. Mahler, *Advances in Statistical Multisource-Multitarget Information Fusion*. Norwood, MA, USA: Artech House, 2014.
[36] A. F. García-Fernández, L. Svensson, and M. R. Morelande, "Multiple target tracking based on sets of trajectories," *IEEE Trans. Aerosp. Electron. Syst.*, vol. 56, no. 3, pp. 1685–1707, Jun. 2020.
[37] D. F. Crouse, "On implementing 2D rectangular assignment algorithms," *IEEE Trans. Aerosp. Electron. Syst.*, vol. 52, no. 4, pp. 1679–1696, Aug. 2016.
[38] S. Yang, M. Baum, and K. Granström, "Metrics for performance evaluation of elliptic extended object tracking methods," in *Proc. IEEE Int. Conf. Multisensor Fusion Integration Intell. Syst.*, 2016, pp. 523–528.
[39] L. G. Khachiyan, "Polynomial algorithms in linear programming," *USSR Comput. Math. Math. Phys.*, vol. 20, no. 1, pp. 53–72, 1980.
[40] P. Corazza, "Introduction to metric-preserving functions," *Amer. Math. Monthly*, vol. 106, no. 4, pp. 309–323, Apr. 1999.
[41] E. Hille and R. S. Phillips, *Functional Analysis and Semi-Groups*. Providence, RI, USA: Amer. Math. Soc., 1957.
[42] K. Granström, L. Svensson, Y. Xia, J. Williams, and A. F. García-Fernández, "Poisson multi-Bernoulli mixtures for sets of trajectories," *IEEE Trans. Aerosp. Electron. Syst.*, vol. 61, no. 2, pp. 5178–5194, Feb. 2025.
[43] J. L. Williams, "Marginal multi-Bernoulli filters: RFS derivation of MHT, JIPDA and association-based MeMBer," *IEEE Trans. Aerosp. Electron. Syst.*, vol. 51, no. 3, pp. 1664–1687, Jul. 2015.
[44] A. F. García-Fernández, J. L. Williams, K. Granström, and L. Svensson, "Poisson multi-Bernoulli mixture filter: Direct derivation and implementation," *IEEE Trans. Aerosp. Electron. Syst.*, vol. 54, no. 4, pp. 1883–1901, Aug. 2018.
[45] B. T. Vo and B. N. Vo, "Labeled random finite sets and multi-object conjugate priors," *IEEE Trans. Signal Process.*, vol. 61, no. 13, pp. 3460–3475, Jul. 2013.
[46] A. F. García-Fernández, L. Svensson, J. L. Williams, Y. Xia, and K. Granström, "Trajectory Poisson multi-Bernoulli filters," *IEEE Trans. Signal Process.*, vol. 68, pp. 4933–4945, 2020.
[47] K. G. Murty, "An algorithm for ranking all the assignments in order of increasing cost," *Operations Res.*, vol. 16, no. 3, pp. 682–687, 1968.
[48] Y. Bar-Shalom, T. Kirubarajan, and X. R. Li, *Estimation With Applications to Tracking and Navigation*. Hoboken, NJ, USA: Wiley, 2001.
[49] Y. Xia, A. F. García-Fernández, J. Karlsson, K.-C. Chang, T. Yuan, and L. Svensson, "Probabilistic GOSPA: A metric for performance evaluation of multi-object filters with uncertainties," *IEEE Trans. Aerosp. Electron. Syst.*, vol. 61, no. 5, pp. 15113–15121, 2025.
[50] Y. Xia, A. F. García-Fernández, J. Karlsson, Y. Ge, L. Svensson, and T. Yuan, "Probabilistic trajectory GOSPA: A metric for uncertainty-aware multi-object tracking performance evaluation," in *Proc. IEEE Int. Conf. Multisensor Fusion Integration Intell. Syst.*, 2025, pp. 1–7.
[51] C. S. Kubrusly, *The Elements of Operator Theory*. Berlin, Germany: Springer, 2011.